Geoscience and Remote Sensing (2019) Vol. 2: 1-24
Clausius Scientific Press, Canada

DOI: 10.23977/geors.2019.21001
ISSN 2523-2592

# *Estimation of Petrophysical Properties of Ajali Sandstone in Western Anambra Basin Using Granulometric Analysis*

**Edirin Akpofure[a, *] Ebiegberi Oborie[b]**
*Department of Geology, Niger Delta University, Wilberforce Island, Bayelsa State, Nigeria.*
[a] *edirinakpofure@yahoo.com* , [b] *ebixl14@mail.com*
**Corresponding Author*

***Keywords:*** Permeability, Porosity, Grain size distribution, Sedimentary structures, Diagenetic Imprints.

***Abstract:*** Most sedimentary deposits have complex regional permeability and porosity variations which can be determined through various methods. The petrophysical properties of Ajali Sandstone such as permeability, porosity, and grain mean diameter were estimated using textural characteristics of the sediment from field data, petrography and grain size distribution. Grain-size distributions of sediment samples were determined by mechanical sieving. The porosity and permeability have been affected adversely by the moderate to poor sorting of grains. Whereas, fracture line, diagenetic imprints such as the solution, alteration and corrosion at grain margins and lack of cement have made the grains friable, thereby, increasing porosity. Sedimentary structures such as the reactivation surfaces and mud drapes which interspace the thick cross-bedded beds form seals which impede permeability. The porosity of the sandstone is very high and ranges mainly from 50% - 70%, with a few above 70%. Whereas, the least estimated permeability is 3.74 m/day and the highest is 724.55 m/day. A very complex variation exist in the permeability of the studied sandstone which may be due to the occurrence of the several large planar, trough and herringbone cross stratification, erosion and pebble lagged surfaces prevalent in the Formation. There is a strong correlation between permeability and porosity and the associated regression equation is expressed, with a correlation coefficient $R^2 = 0.6795$. Poor correlations exist between permeability and other grain size parameters such as grain mean diameter, $d_{10}$ and $d_{60}$.

## Introduction

The Ajali Sandstone is a major clastic lithologic unit in the Anambra Basin which resulted from the tectonics and structure of the Benue Trough during the Santonian event. The earliest and dominant deposits were the proto delta suite which is majorly Cretaceous. The Basin is partly sandwiched between the southern Benue Trough above and the Niger Delta Basin below. The Campanian – Maastrichtian proto delta sediments in the Basin include the Nkporo Group, Mamu Formation, Ajali Formation and the Nsukka Formation. The Ajali Sandstone is sandwiched between the Mamu Formation and the Nsukka Formation - the lower and upper coal measures respectively. Regionally, the Sandstone comprises of thick successions of sandstones with thin beds of mudstone and shales near the base. The Formation is extensively cross-stratified into different types of cross-bedding including: planar, trough and herringbone cross-bedding which occur at different stratigraphic levels. The cross-beds are large scale (over 1 m high in places). Initially, the Formation was called the White False Bedded Sandstone and later changed to Ajali Sandstone (Reyment, 1965).

The Ajali Sandstone is whitish in colour with some few siltstone and clay intercalations, and it is extensively exposed with an average exposed height of about 11 m in the study area. It is already weathered on the surface. The thicknesses of the beds are not uniform but occur as parallel low dipping beds. The beds consist of friable, moderately sorted sands with shape of grains ranging from subangular to subrounded (Reyment, 1965; Kogbe, 1976).

The petrophysical properties of the Ajali sandstone, such as its porosity, permeability and mean grain diameter which equates its surface area are estimated in this study from grain size analysis.

Ayogwiri, Fugar and Orame where the study outcrops occur are situated in Etsako West Local Government Area of Edo State, Nigeria. The area is covered by the Ajali Sandstone. Accessibility to and within the study area is fairly good. There are good network of tarred roads including Auch-Ibillo road, Auchi-Agenebode road among others. The Sandstone exposures in the area are along road cuts and in quarries.

## Previous Studies

Simpson (1955) described the Ajali Sandstone as "False Bedded Sandstone", that consists mainly of fine-grained, friable, sub-angular to sub-rounded Sandstone. Jones and Hockey (1964) classified the Sandstone as part of the Upper Coal Measure, while Kogbe (1976) shows that the Ajali Sandstone in western Nigeria is the lateral equivalent of Ajali Sandstone of eastern Nigeria. Rahaman (1976a) also mapped the area and grouped the Sandstones as part of the False Bedded Sandstone within the coal measure belt.

The unit stratotype of Ajali Sandstone was examined by Reyment (1965), and observed that the Formation lies between two parallic sequence; the underlying Mamu Formation and the overlying Nsukka Formation thus suggesting a continental origin. However Hoque and Ezepue (1977) changed this line of thought by suggesting a fluvial-deltaic environment for the Sandstone in the Anambra Basin.

Amajor (1987) did facies analysis of the Ajali Sandstone in the Okigwe area and subdivided the Formation into two fining upward sequences, with each possessing three sub-facies. He discovered that the Ajali Formation which was formerly regarded as a continental environment contains marginal deposits at the base of the area. As a result, he assigned a fluvial-marine depositional environment.

Ladipo (1988a), found that the sandstone bodies in the south eastern Nigeria had shapes ranging from sheetlike, lobate, lenticular and elongate forms deposited in a wide variety of depositional setting, such as deltas and flood plain channels, shallow marine, shelves, shorelines etc. He further said the process regime of the environment, nature of sediment supply and shoreline behaviour was responsible for the shape of the sand bodies.

Ladipo, (1986a, b and 1988b), using process interpretation of sedimentary structures and palaeocurrent analyses from the Ajali Sandstone suggested a tidally influenced regime possibly a tidal shelf characterized by shoreline – parallel sand bodies with intercalations of mud.

Akpofure and Etu-Efeotor (2013a, 2013b)) using data from several sedimentary structures, biostratigraphy and granulometric analysis inferred fluvial and shallow marine (Shoreface) environments with very strong and extensive tidal influences.

Petrographic studies of the Ajali Sandstone by Akpofure and Etu-Efeotor (2013a) show the dominant mineral is quartz which is above 95%, with very minimal feldspar in places. The matrix is made up of smaller quartz grains that may have fractured from the larger grains. They also inferred that the Ajali Sandstone may have been indurated initially and due to severe compaction, dissolution, intense alteration and corrosion, especially at grain margin, recrystallization and replacement, have become friable over time, making it susceptibility to erosion.

Akpofure and Akana (2015) infer the Ajali Sandstone is made up of two basic facies. The basal facies, made up of thinly laminated, heterolithic beds of the shoreface environment, - The upper facies consists mainly of cross-bedded sandstones -.The major palaeocurrent direction of the Ajali Sandstone in the studied area was in the NE direction which infers the sediment provenance source to be the uplifted Abakiliki Anticlinorium. However, subordinate direction to the south occurs in Orame (Akpofure and Akana, 2015).

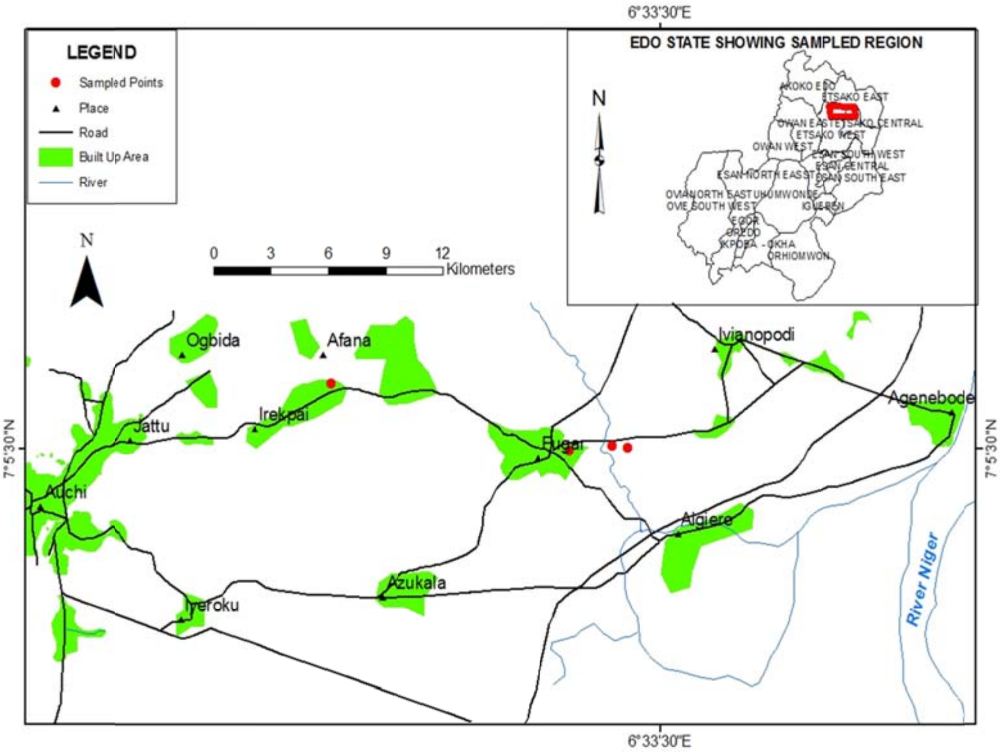


Figure 1: Location map showing sample points in Ayogwiri, Fugar and Orame.

## Materials and Methods

Two methods were employed: Outcrop sampling and laboratory analysis. During the outcrop sampling, field data and samples were taken from outcrops at quarries and road cuts using field equipment such as compass clinometers, tape for measuring bed thickness, hammer and sample bags for collecting and bagging samples were some of the materials used. Sampling methods by Tucker (1988) and Nwajide and Reijers (1996) were adopted. Samples were further prepared and presented for granulometric analysis. Twenty – eight (28) samples of unconsolidated sandstone which were oven dried and passed through a set of sieves with diameters ranging from 0.075mm to 2mm and shaken by a Ro–Tap Shaker. Graphical methods adopted for deducing textural parameters are as given by Folks and Ward 1957 with the Wentwort scale for particle size distribution. Textural parameters deduced were used for calculating porosity, permeability and grain mean diameter. Vukovic and Soro (1992) was used for porosity and Kozeny – Carman equation for permeability.

The general mathematical expressions for calculating the geometric mean diameter $D_m$ of samples is given below:

$Dm = Exp [ 1/M \sum mi \ln(d_{ig}) ]$ (1)

M = mass of the sample, mi = mass of particular sieve residue E

$d_{ig}$ = Square root of di< x di> (2)

di< = smallest and di> largest grain sizes. (Geometric mean of rated size of adjacent sieves)

Porosity $\eta = 0.255 (1 + 0.83u)$ (3) (Vukovic and Soro, 1992).

Porosity derived from the empirical relationship between porosity and the coefficient of grain uniformity ($\mu$)

$\mu$ = Coefficient of uniformity (4)

$d_{60}/d_{10}$ Here, $d_{60}$ and $d_{10}$ are the sieve diameters in (mm) for which 60% and 10% of the sample will pass respectively.

Permeability/hydraulic conductivity

$k = n^3 / 180(1 - \eta)^2 D^2{}_m$ (5) (Kozeny – Carman)

K = Permeability, $\eta$ = porosity, $D_m$ = geometric mean grain diameter

## Results and Interpretation

### Lithologic Description of the Sandstone

The Sandstone, outcrops in Ayogwiri at a quarry site in the village at a point with a geo-reference of $07^o$ 7.230' N and $06^o$ 24.217'E. Eight beds separated by thin beds of mud are observed containing various geological structural imprints (Figure 2). Bed A is made up of near horizontal, thin laminated beds of fine sands and silt with flaser bedding and grayish clay lenses. It is about 37 cm thick. Bed B, 216 cm thick is heterolithic and made up of near horizontal layers of beds striking 340 NW with dip of $6^o$. Bed B exhibits cyclic sedimentation of fine, brown sands and clay beds at intervals. Bed B is capped by a clay bed of about 6 cm thick. Bed C, 153 cm thick, overlies Bed B.

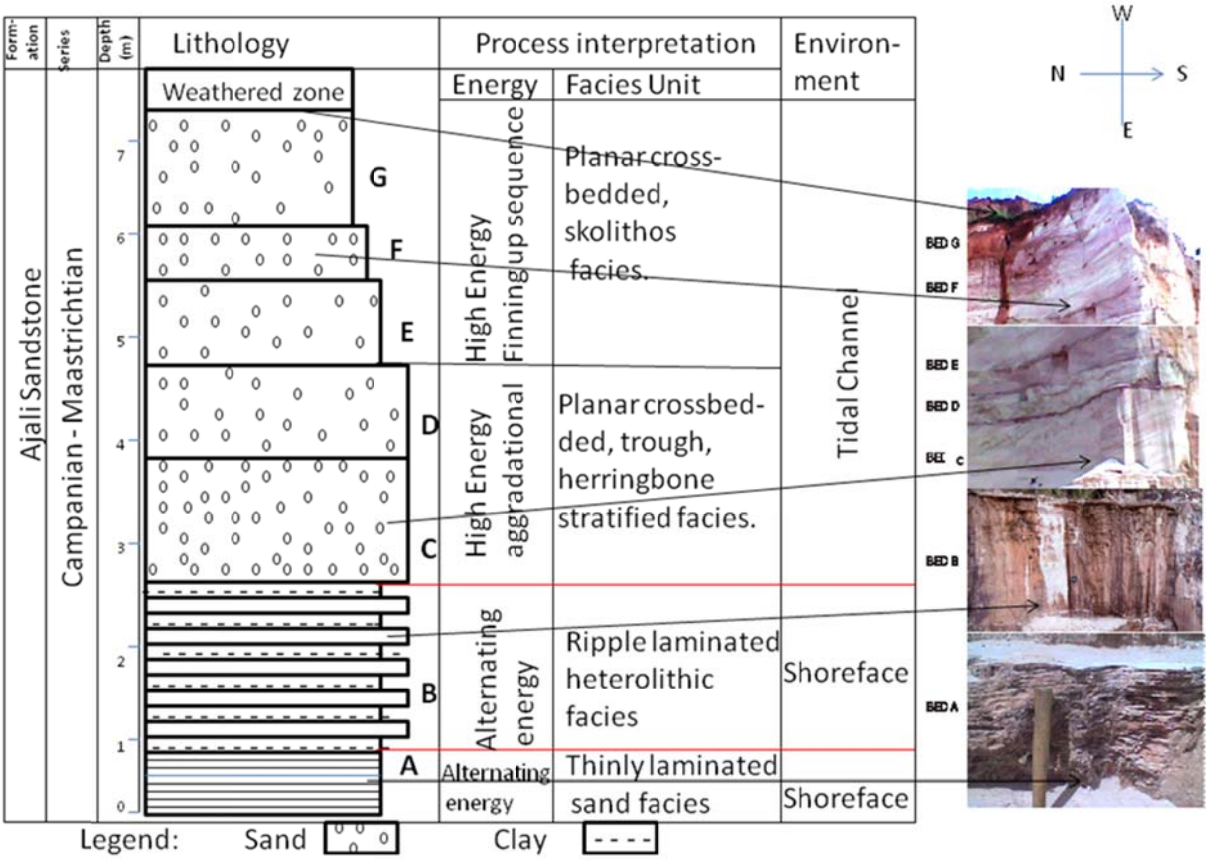


Figure 2: Stratalog of Ajali Sandstone in Ayogwiri

The sand is white and friable, medium to coarse grain, with pebbles at the base and in places. Large planar cross-beds and clay lenses occur. It is also capped by a mud drape that is about 6 cm thick. Bed D, 118 cm, is a composite bed with planar, trough cross-beds, herringbone structure and varying palaeocurrent directions. Three major current directions observed are in the NE, SE and NNW, with that in the NNW most prominent (Akpofure and Akana 2015). The bed is also capped by a mud drape of 6 cm thick. Bed E, 68 cm thick was deposited with large planar cross-beds. Beds D and E are made up of whitish medium to coarse grain sands, with pebbles in places. Bed F has white, fine to medium grain sands with large planar cross-beds. Bed G overlies bed F, the grains are also white, fine to medium grain sands but massive without cross-beds. The weathered zone lies above bed G, it is about 130 cm thick and it is highly lateritic and most part of it is ironstone. (Akpofure and Akana 2015)

Deposition of the Ajali Sandstone in Fugar took place in the form of packets or bundles of curved inclined beds of short lateral extent. The location of outcrop logging in Fugar is along a road cut on Auchi – Fugar- Agenebode road at a geo-reference of 07$^{o}$ 05.448'N and 006$^{o}$ 30.943'E. At this location, several bundles of large inclined cross-beds known as epsilon beds formed from the lateral migration of pointbars were observed (Figure 3). The bundle planes are erosion surfaces. The thickness of each bed of the epsilon bundles ranges from 2 cm to 5 cm, with average of about 3.4 cm with laminations within them (Akpofure and Akana 2015).

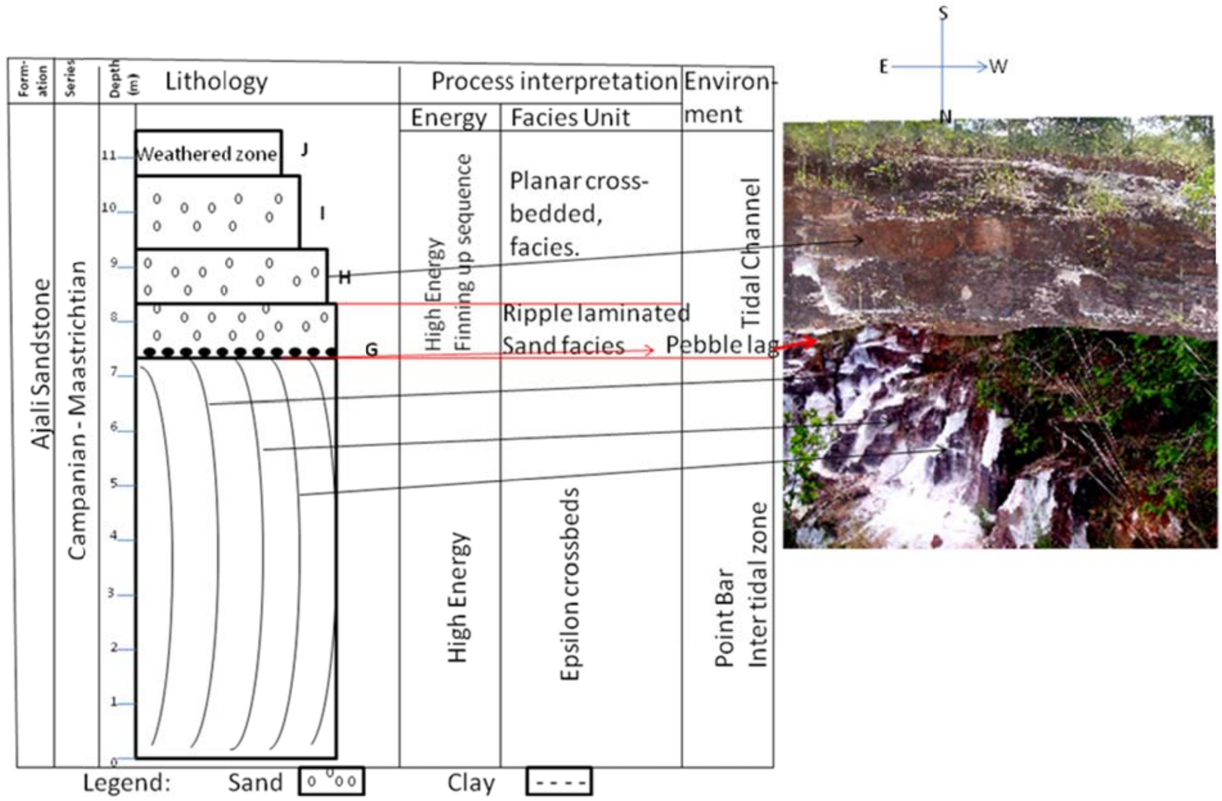


Figure 3: Stratalog of Ajali Sandstone at Fugar.

The height of the Sandstone at this exposure is 12.5 m. From the bottom to 7.2 m, there are several packets of epsilon beds. Epsilon Bed A is 27 cm thick. The grains are fine and light brown. Epsilon Beds B and C are 117cm and 170 cm high respectively. The sands are fine grain. The epsilon Beds D, E and F have medium to coarse grain sands and heights of 160 cm, 130 cm and 110cm respectively.

The epsilon beds are overlain by Bed G. The surface separating Bed G from the epsilon bundles is an erosion surface lagged with pebbles. Bed G is ripple laminated and 80 cm high. It is overlain by Bed H, 110 cm high with large planar cross-beds and pebbles occurring in places. Above Bed I is Bed H; it is 150 cm thick and fine to medium grain. Also, Bed J is fine to medium grain and 120cm thick.

Ajali Sandstone is massively exposed along the road cut in Orame village along Agenibode road, at a point with a geo-reference of 07$^{o}$ 05.576'N and 06$^{o}$ 32.593'. The sand body is as high as 13.05 m. The beds occur as near horizontal cross-beds. Fifteen of such beds occur with the last severely weathered. The height of each bed is indicated in the stratalog (Figure. 4).

The first two beds, A and B, are separated by thin mud layer each have cyclic sedimentation with the deposition of thin sand and clay beds and granules in places. They are both heterolithic. Bed B is overlain by a thick clay bed 23 cm thick. The clay bed is thinly laminated. Bed C is massive and structure-less with medium grain sands while, Bed D has convolute deformational folds with light brown medium - coarse grains. The sands of both Beds E and F are white medium grains but Bed F has large planar cross-beds. Bed G is fine grain, white, with granules occurring in places, it also has large planar cross-beds. Bed H has convolute deformational folds, white, fine to medium grain with pebbles. Bed I is medium to coarse grain and light brown in colour. Above Bed I, are Beds J and K which are fine grain sands. Large planar cross-beds occur in Beds I and J.

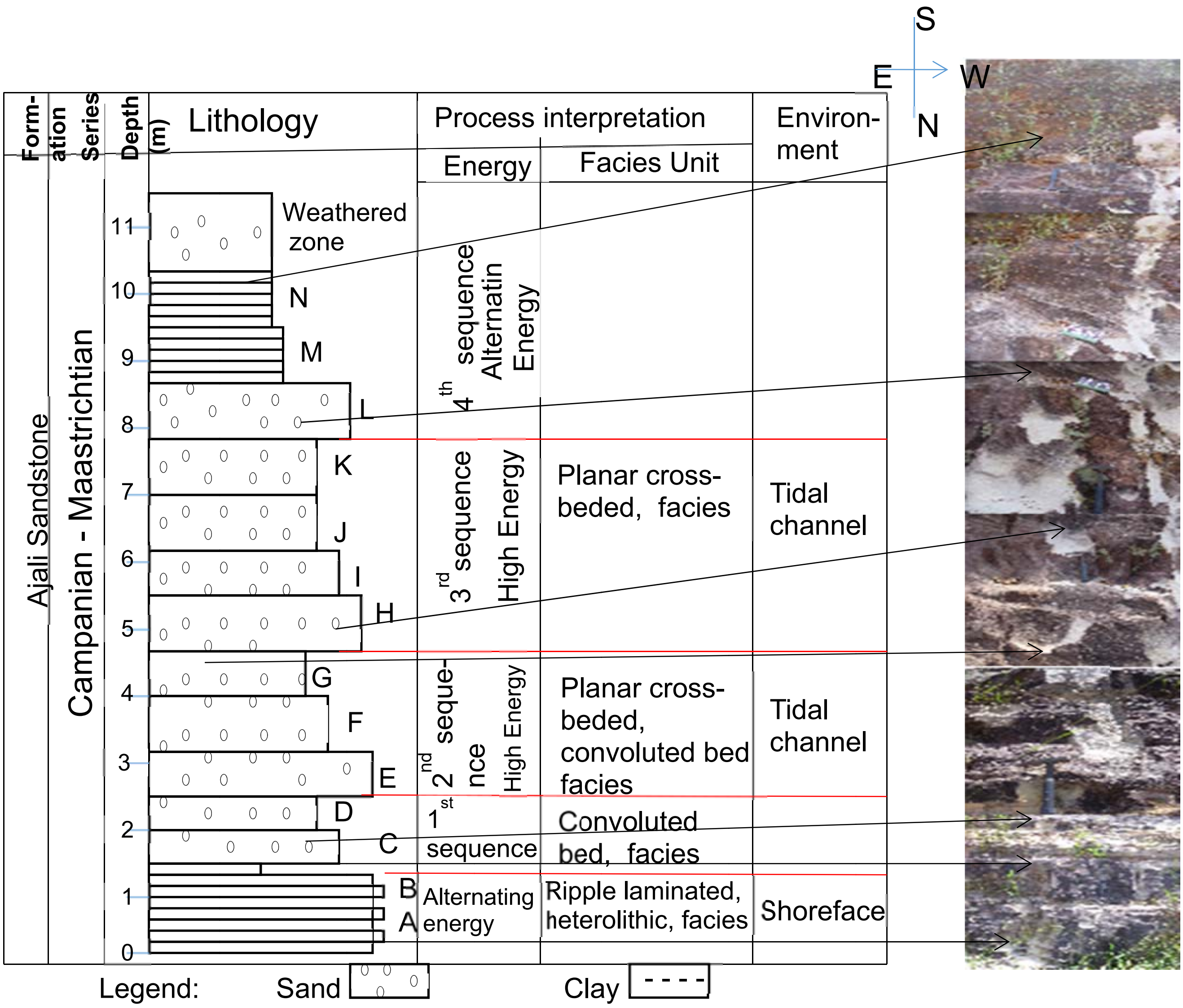


Figure 4: Stratalog of Ajali Sandstone in Orame.

## Photomicrographs of the Sandstone Samples from Ayogwiri

At Ayogwiri, samples taken from Beds A and B show fine quartz grains which are generally subangular to angular. The beds are heterolithic, with moderately to poorly sorted layers with pebble grains in places. The large pebble grains are subrounded and show clear grain margins. Stress zones and fracture lines are not common on these grains. The surface of the grains are smooth with no etching. Most of the quartz grains are monocrystalline showing straight margins. Iron oxide coating is seen on some of the grains, The mineral glauconite occur and inclusions were also seen (Figure 5 – 7, Akpofure and Etu-Efeotor 2013a)

In between each of the beds are thin silty beds that average about 5 cm in thickness, these are mudrapes. These beds contain fine-grained sands with so much fracture lines, alteration and corrosion of grain margins. Most of the surfaces are etched. Iron oxide coating is very common coat on the quartz grains. (Akpofure and Etu-Efeotor 2013a)

The cross-bedded facies of the Ajali Sandstone in Ayogwiri have grains that are subangular to angular, moderately to poorly sorted beds. They show monocrystalline and polycrystalline quartz grains. Authigenic quartz is seen as quartz overgrowth (Figure 6). Most of the grain margins show alteration and corrossion. Stress zones and shadows were also noticed on the grains (Akpofure and Etu-Efeotor 2013a)

### Photomicrographs of the Sandstone Samples from Fugar

Most of the grains of the Sandstone at this location are monocrystalline but polycrystalline quartz also occurs. The sands are moderately to poorly sorted, sub rounded to rounded grains. Most have clear margins, though a few samples are with corroded margins. Inclusions and alterations occur mainly within the grains. Cast of biogenic forms such as *Reophax sp, Haplophragmoides sp* occur in thin section. Infiltration of hollow molds with quartz mineral was also observed. Authigenic quartz occurs as microcrystalline grains formed in situ (Figures 8 – 10, Akpofure and Etu-Efeotor 2013a)

### Photomicrographs of the Sandstone Samples from Orame

Similar features found in previous locations were also recorded in Orame: Inclusions, alteration and corrosion at grain margins, fracture lines, stress shadows, authigenic quartz. Rotation of some grains was observed. Iron oxide is seen coating some of the grains. Fracture lines, though present were not as common. The grains are mainly moderately sorted to poorly sorted. Most have sharp grain margins with corrosion of margins occurring in some. Some sections have sub angular grains while others were subrounded (Figures 11 – 15, Akpofure and Etu-Efeotor 2013).

Petrophysical properties of sediments such as porosity and permeability are usually controlled by textural characteristics of that deposit at deposition. Diagenetic changes such as compaction, cementation, solution, alteration etc after deposition also influence by either increasing or decreasing porosity and permeability.

The Ajali Sandstone is a quartz arenite, quartz constitutes above 95% of framework elements. The matrix is made up finer grains of quartz (figures 8 – 15). The fabric is not cement supported as a result, the Ajali Sandstone is very friable. Most of the grains are subangular to angular which favour high porosity. Permeabilty increases with increase in grain size, while porosity increases with increase sorting. The Sandstone is moderately to poorly sorted. Also the grains record several diagenetic imprints: Authigenic quartz overgrowth is common, which tends to decrease pore space, thereby decreasing porosity, but others such as solution and alteration at grain contacts increase pore spaces and invariably increase porosity. Fracture lines that are prevalent in the grains may also have contributed to increased porosity. Also inferred is the complex variation in permeability caused by the large planar, trough and herringbone cross stratification, erosion and pebble lagged surfaces prevalent in the Formation.

## Textural Characteristics

The population of the sediments of Ajali Formation is separated slightly and the size frequency distribution departs markedly from the log normality. The composite population is markedly skewed with a secondary modal class in some beds in the coarse sand (-1-0) on the phi scale. The main population of the distribution lies between percentile 30 and 60 with the primary modal class 5-6 grade on the phi scale. According to Visher (1969), the sediments of Ajali Sandstone are attributed to saltation and suspension transports (Figures 16 -22). Graphic mean of samples from Ayogwiri range from 3.2 to 5.03; that is fine sand to coarse silt, but they are predominantly medium to fine grain sands. The mean is 3.80; reflective of the very fine sand fraction for the sandstone. That for the Sandstone at Fugar is 3.65 which is a reflection of very fine sands but sample population range from 2.6 to 4.03. Orame is predominantly very fine sands with an average of 3.78 and a population range of 3.3 to 3.9. The sediments in Ayogwiri range from mesokurtic to very leptokurtic. None is platykurtic and three are mesokurtic. It is predominantly leptokurtic. Fugar and Orame range from leptokurtic to very leptokurtic. None of the sediments showed platykurtic or mesokurtic kurtosis (Akpofure and Etu-Efeotor 2013b).

The average values of the grain size parameters of Ajali Formations in the study area are as follows: Mean 3.80; Sorting 0.92 (moderately sorted); Skewness -0.27 (negatively skewed); Kurtosis 1.41 (leptokurtic); Median 4.03; Coefficient of variation 0.05; Phi deviation 0.83 (Table 1, Akpofure and Etu-Efeotor 2013b).

TABLE 1: AVERAGE VALUES OF GRAIN SIZE PARAMETERS OF AJALI FORMATION (AKPOFURE AND ETU-EFEOTOR 2013 b).

| S/N | LOCATION | MEAN | SORTING | SKEWNESS | KURTOSIS | MEDIAN | COFF. OF VARIATION | PHI DEVIATION |
|---|---|---|---|---|---|---|---|---|
| | AYOGWIRI | 3.98 | 0.86 | -0.31 | 1.26 | 4.41 | 0.71 | 0.82 |
| | FUGAR | 3.63 | 0.98 | -0.23 | 1.35 | 3.81 | 0.3 | 0.95 |
| | ORAME | 3.78 | 0.91 | -0.49 | 1.58 | 3.87 | -0.87 | 0.73 |
| AVERAGE | | 3.80 | 0.92 | -0.27 | 1.41 | 4.03 | -0.05 | 0.83 |

## Photomicrographs of Ajali Sandstone in Ayogwiri (Akpofure and Etu-Efeotor 2013)

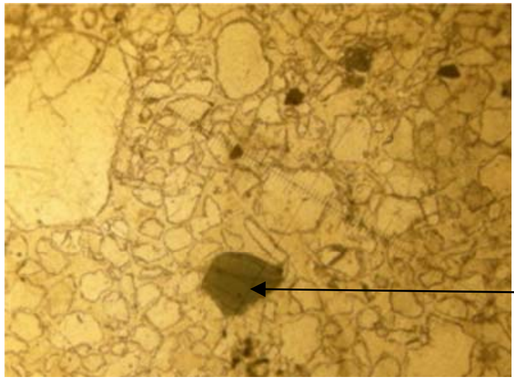


PPL.

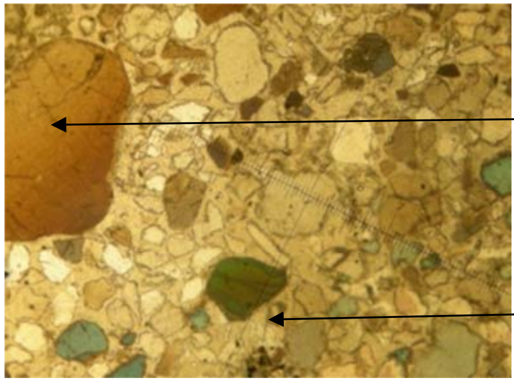


XPL

Fig. 5: Poorly sorted, sub rounded grains. Iron oxide coating on quartz grain, Glauconite grain (G)

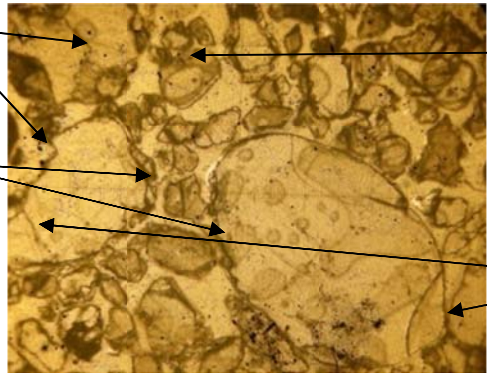


PPL.

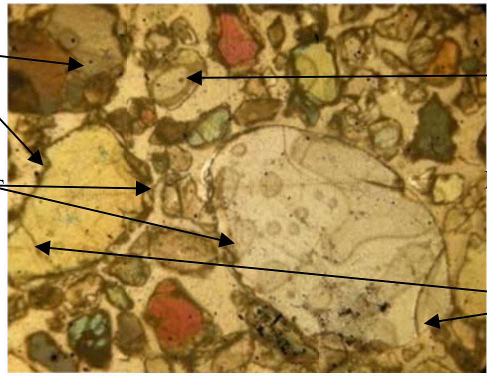


XPL

Fig. 6: Stress zonation (SZ), Corrosion and alteration at grain margins (ALT); Sutured contact in polycrystalline grain (SC); Quartz overgrowth (QO).

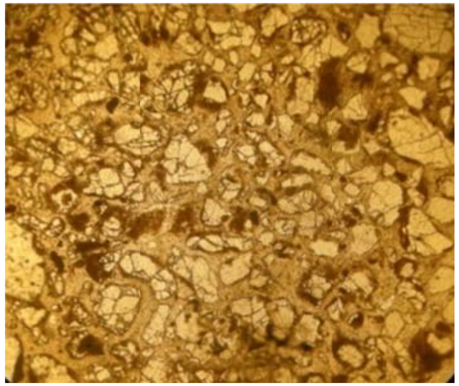

PPL.

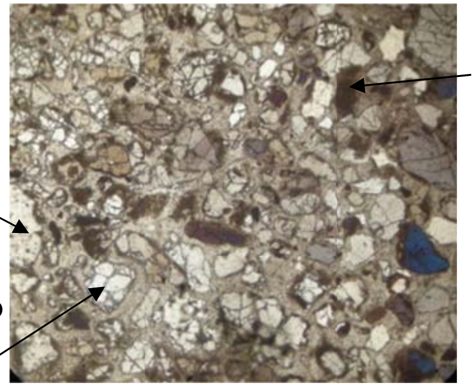


XPL

Fig. 7: (Mudrape): Severely fractured grains; Iron oxide coating on quartz grains, Fractured quartz (FQ), Etch marks (EM).

## Photomicrographs of Ajali Sandstone in Fugar (After Akpofure and Etu-efeotor 2013)

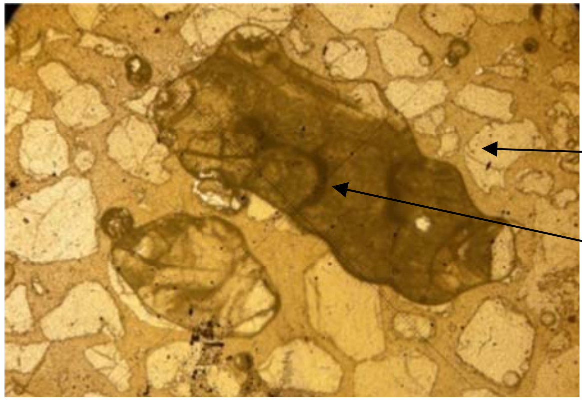


PPL

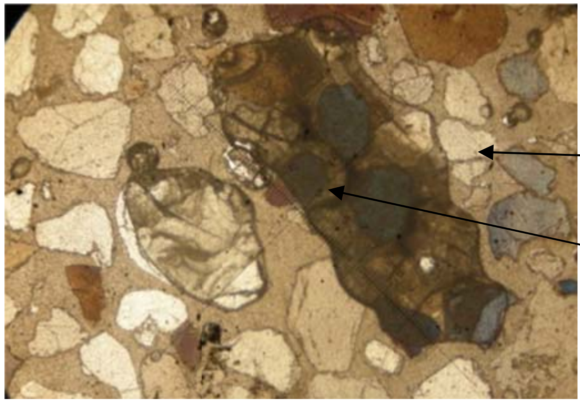


XPL

Fig. 8: -Biogenic form (BF) – *Haplophragmoides sp.* Quartz overgrowth (QO).

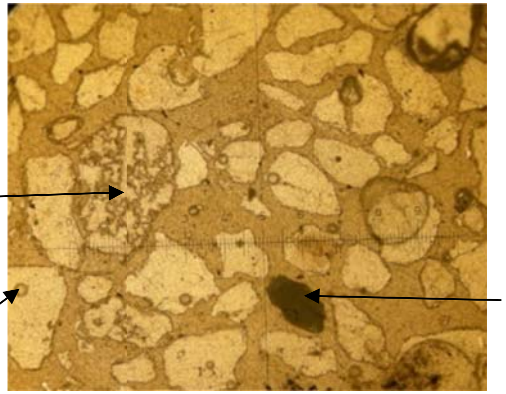


PPL

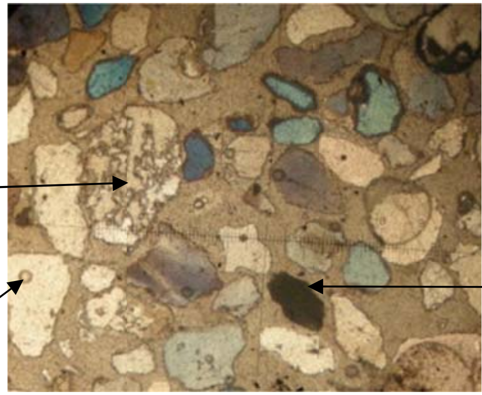


XPL

Fig. 9: Monocrystalline qtuatz grains, Alteration (ALT) and disintegration or collapse of grain, Inclusions (I), glauconite (G) Grains are moderately sorted.

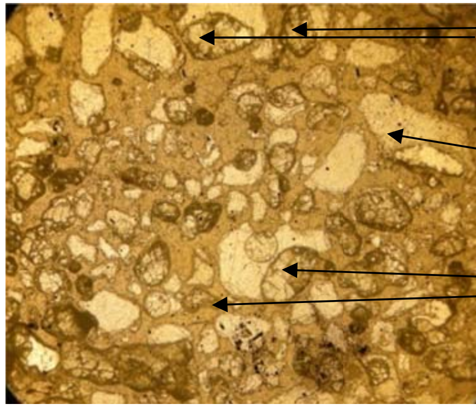


PPL

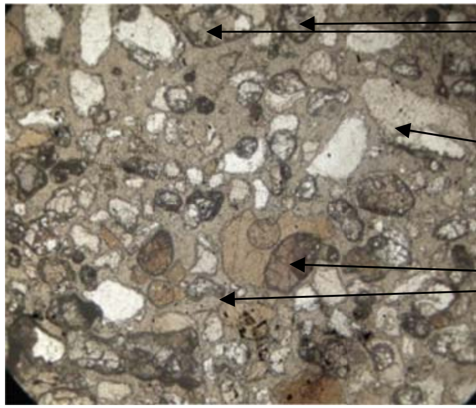


XPL

Fig. 10: -Polycrystalline quartz, -Biogenetic form (BF) –*Reophax sp.* poorly sorted grains. -Alteration of Qtz grain, Reaction rims with corrosion at margins, Hollow cast (HBC).

## Photomicrographs of Ajali Sandstone in Orame (Akpofure and Etu-Efeotor 2013)

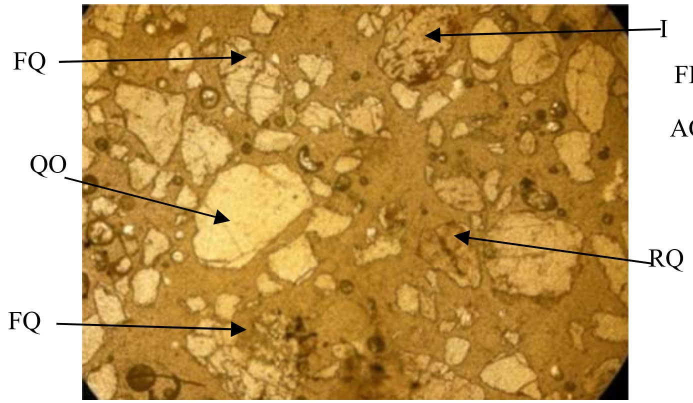


PPL

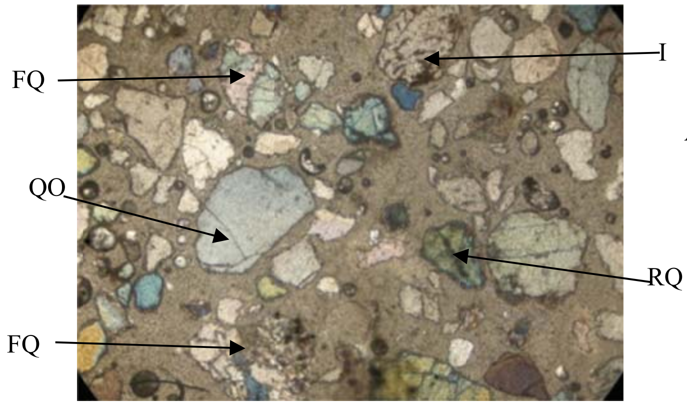


XPL

Fig 11: Alteration and reaction at rims, fractured quartz grain into smaller grains (FQ), Rotated grain (RQ)

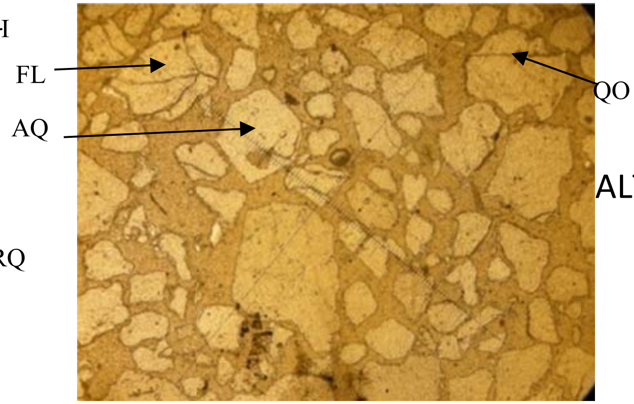


PPL

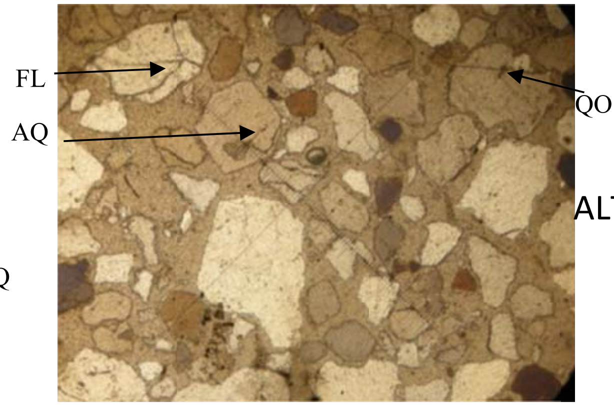


XPL

Fig 12: Subangular grains with fracture line (FL), Authigenic quartz (AQ) and Quartz overgrowth (QO).

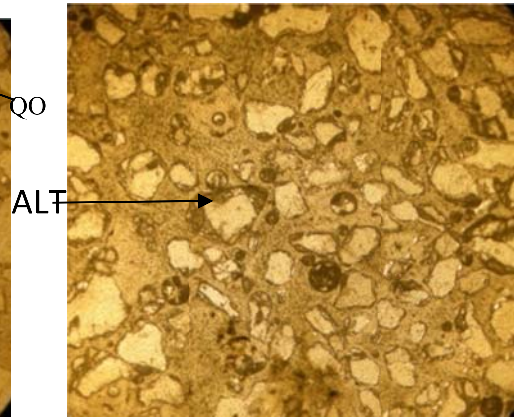


PPL

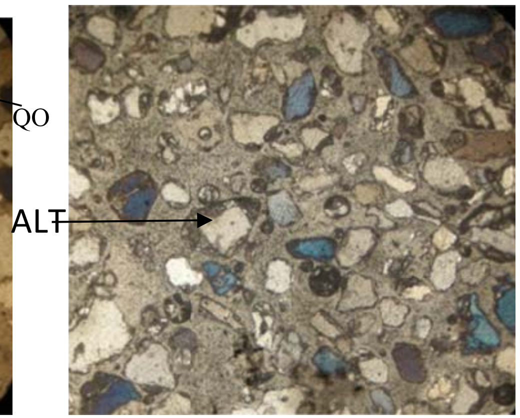


XPL

Fig 13: Angular grains, moderately sorted, large quartz grain. movement of alteration (ALT) and reactions rims from grain margins towards the center.

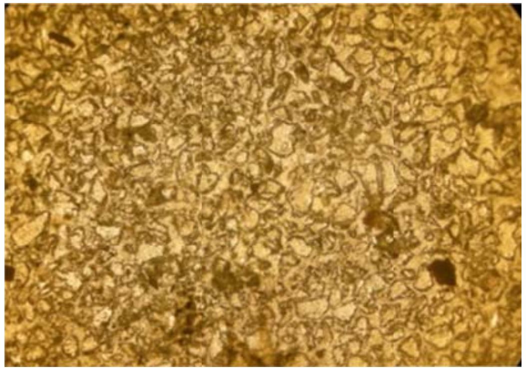

PPL

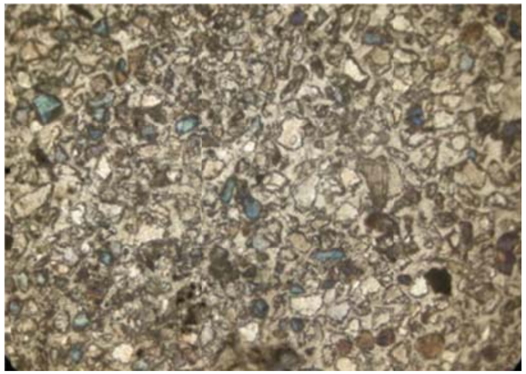

XPL

Fig 14: Dissolution, alteration and recrystallization at margins of fine grain

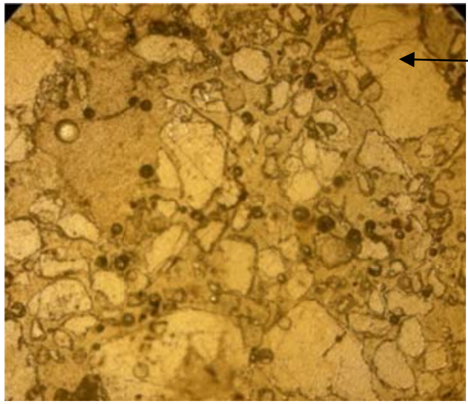

PQ

PPL

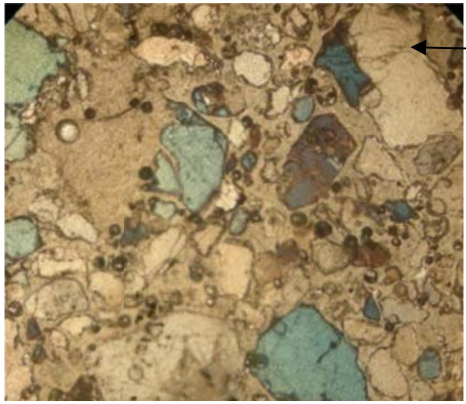

PQ

XPL

Fig 15: Very coarse angular grains, Polycrystalline quartz (PQ).

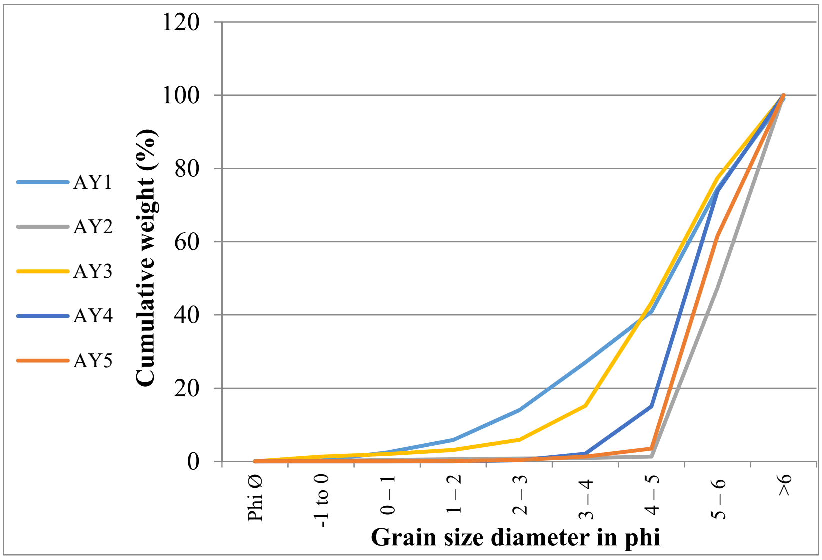


Figure 16: Cummulative weight versus grain-size diameter in phi in Ayogwiri.

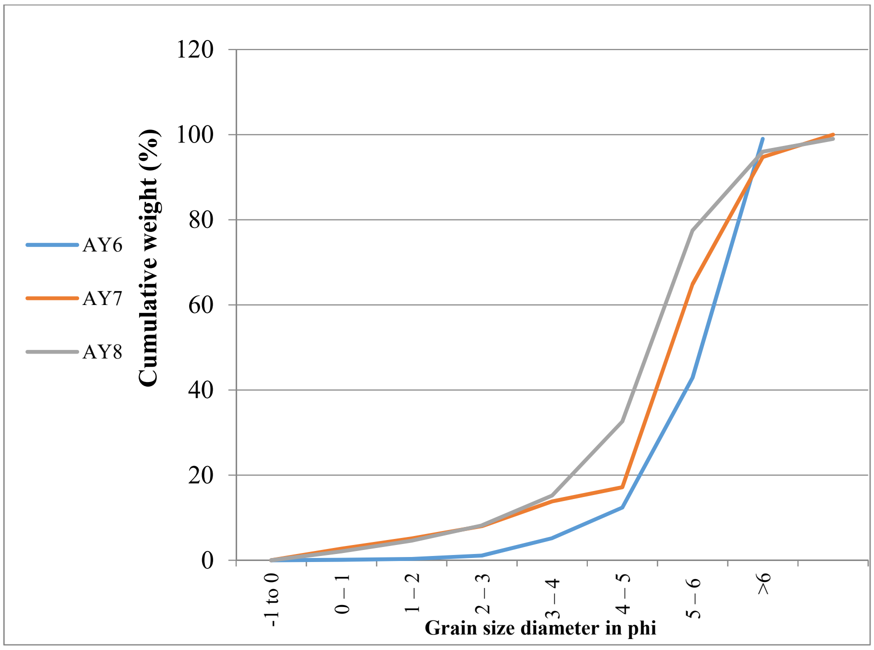


Figure 17: Cummulative weight versus grain-size diameter in phi in Ayogwiri.

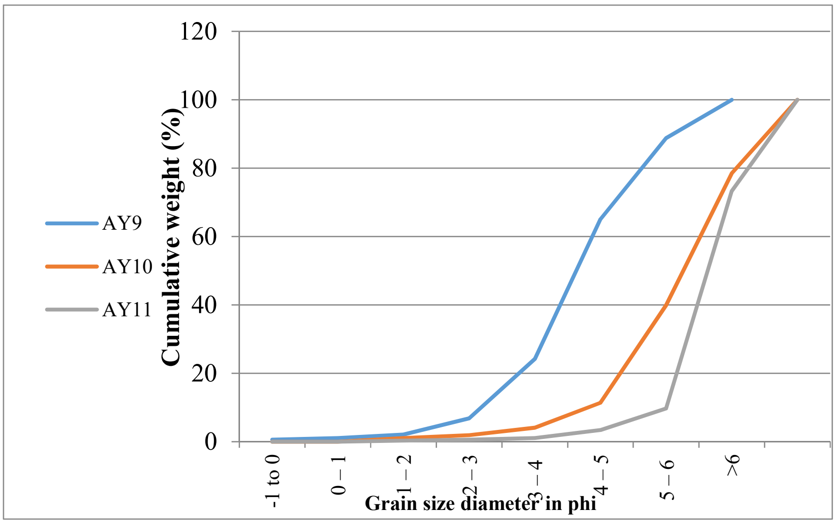


Figure 18: Cummulative weight versus grain-size diameter in phi in Ayogwiri.

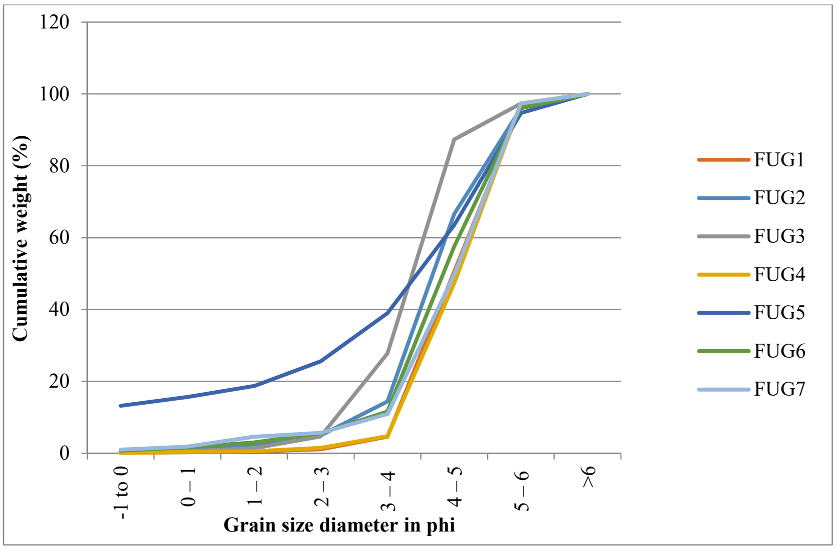


Figure 19: Cummulative weight versus grain-size diameter in phi in Fugar.

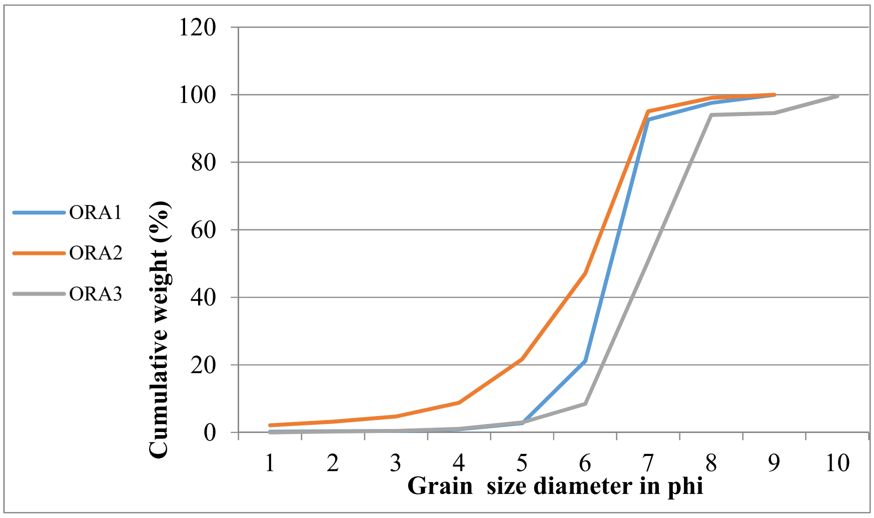


Figure 20: Cummulative weight versus grain-size diameter in phi in Orame.

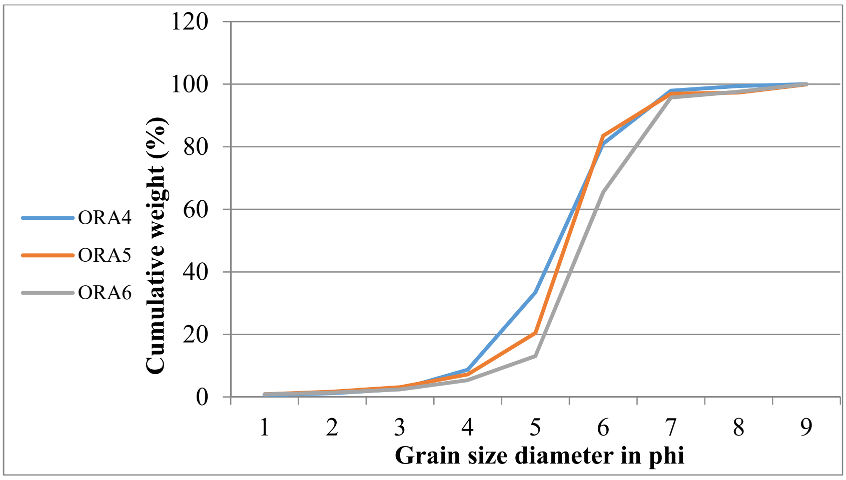


Figure 21: Cummulative weight versus grain-size diameter in phi in Orame.

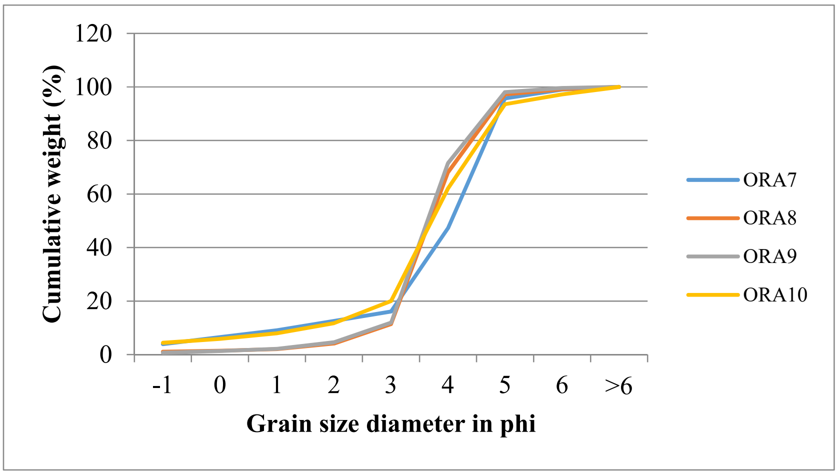


Figure 22: Cummulative weight versus grain-size diameter in phi in Orame.

Table 2: PETROPHYSICAL PARAMETERS OF AJALI SANDSTONE IN WESTERN ANAMBRA BASIN.

| Location | | Samples | D10 | D60 | Coefiient of uniformity $\mu$ = d60/d10 | Porosity $\eta$ = 0.255(1+0.83$\mu$) | Dig = square root of di< x di> | Mean grain diameter Dm | Square of Mean grain Diameter $D^2$m | Permeability K=mm/s | Permeability K=mm/s | Permeability K= m/day |
|---|---|---|---|---|---|---|---|---|---|---|---|---|
| Bed A | | Ayo 1 | 1.6 | 4.8 | 3.00 | 0.905 | 0.387 | 0.4288 | 0.1838 | 0.08386 | 83 x10$^{-3}$ | 724.55 |
| MD b/w AB | | Ayo 2 | 4.6 | 5.1 | 1.11 | 0.495 | 0.387 | 0.3870 | 0.1497 | 0.0003955 | 39 x 10$^{-5}$ | 3.42 |
| Bed B | | Ayo 3 | 2.2 | 4.6 | 2.09 | 0.708 | 0.387 | 0.3873 | 0.1500 | 0.003468 | 34 x 10$^{-4}$ | 29.96 |
| Bed B | | Ayo 4 | 3.7 | 4.7 | 1.27 | 0.53 | 0.387 | 0.3884 | 0.1509 | 0.0005647 | 56 x 10$^{-5}$ | 4.88 |
| Bed B | | Ayo 5 | 4.35 | 5 | 1.15 | 0.504 | 0.387 | 0.3870 | 0.1497 | 0.0004328 | 43 x 10$^{-5}$ | 3.74 |
| MD b/w BC | | Ayo 6 | 2.3 | 3.9 | 1.70 | 0.622 | 0.387 | 0.4639 | 0.1818 | 0.001701 | 17 x 10$^{-4}$ | 14.7 |
| Bed C | | Ayo 7 | 1.3 | 3.9 | 3.00 | 0.905 | 0.387 | 0.3877 | 0.1503 | 0.068577 | 68 x 10$^{-3}$ | 592.51 |
| Bed D | | Ayo 8 | 1.3 | 3.6 | 2.77 | 0.855 | 0.387 | 0.3892 | 0.1514 | 0.02500 | 25 x 10$^{-3}$ | 216 |
| Bed E | | Ayo 9 | 3.8 | 5.2 | 1.37 | 0.551 | 0.387 | 0.3873 | 0.1500 | 0.0006916 | 69 x 10$^{-5}$ | 5.98 |
| Bed F | | Ayo10 | 2.95 | 4.6 | 1.56 | 0.593 | 0.387 | 0.3884 | 0.1509 | 0.001055 | 10 x 10$^{-4}$ | 9.12 |
| Bed G | | Ayo11 | 3.5 | 4.8 | 1.37 | 0.55 | 0.357 | 0.3570 | 0.1275 | 0.000581 | 58 x 10$^{-5}$ | 5.02 |
| Total | | | | | | 0.656 | | 0.395 | | | | |
| | | | | | | | | | | | | |
| Epsilon | | Fug 1 | 3.3 | 4.2 | 1.27 | 0.53 | 0.387 | 0.3884 | 0.1509 | 0.000563 | 56 x 10$^{-5}$ | 4.86 |
| Epsilon | | Fug 2 | 2.7 | 3.9 | 1.44 | 0.567 | 0.387 | 0.3873 | 0.1500 | 0.0008103 | 81 x 10$^{-5}$ | 7 |
| Epsilon | | Fug 3 | 2.4 | 3.6 | 1.50 | 0.58 | 0.387 | 0.3877 | 0.1503 | 0.00614 | 61 x 10$^{-4}$ | 53.05 |

| | | | | | | | | | | | | |
|---|---|---|---|---|---|---|---|---|---|---|---|---|
| Epsilon | | Fug 4 | 3.3 | 4.3 | 1.30 | 0.536 | 0.387 | 0.3884 | 0.1509 | 0.003973 | 39 x $10^{-4}$ | 34.33 |
| Pebble lag b/w Epp and G | | Fug 5 | 2.4 | 3.9 | 1.63 | 0.607 | 0.387 | 0.3884 | 0.1509 | 0.008044 | 80 x $10^{-4}$ | 69.5 |
| Bed G | | Fug 6 | 2.8 | 4 | 1.43 | 0.564 | 0.387 | 0.3873 | 0.1500 | 0.0007866 | 78 x $10^{-5}$ | 6.8 |
| Bed H | | Fug 7 | 2.9 | 4.15 | 1.43 | 0.564 | 0.387 | 0.3881 | 0.1506 | 0.0007897 | 78 x $10^{-5}$ | 6.82 |
| Total | | | | | | 0.564 | | 0.387 | | | | |
| | | | | | | | | | | | | |
| Bed A | | Ora 1 | 3.6 | 4.6 | 1.28 | 0.53 | 0.387 | 0.39039 | 0.15240 | 0.0057032 | 57 x $10^{-4}$ | 49.28 |
| Bed C | | Ora 2 | 2.4 | 4.2 | 1.75 | 0.634 | 0.387 | 0.38720 | 0.149920 | 0.001584 | 15 x $10^{-4}$ | 13.69 |
| Bed D | | Ora 3 | 3 | 4.2 | 1.40 | 0.558 | 0.387 | 0.39842 | 0.15874 | 0.000784 | 78 x $10^{-5}$ | 6.77 |
| Bed E | | Ora 4 | 2.2 | 3.6 | 1.64 | 0.609 | 0.387 | 0.39031 | 0.152348 | 0.001254 | 12 x $10^{-4}$ | 10.83 |
| Bed F | | Ora 5 | 2.3 | 2.7 | 1.17 | 0.509 | 0.387 | 0.39123 | 0.15306 | 0.0019293 | 19 x $10^{-4}$ | 16.67 |
| Bed G | | Ora 6 | 2.5 | 3.9 | 1.56 | 0.593 | 0.387 | 0.38885 | 0.15120 | 0.001070 | 10 x $10^{-4}$ | 9.24 |
| Bed H | | Ora 7 | 1.5 | 4.1 | 2.73 | 0.847 | 0.387 | 0.38701 | 0.14972 | 0.021592 | 21 x $10^{-3}$ | 186.55 |
| Bed I | | Ora 8 | 2.9 | 3.8 | 1.31 | 0.538 | 0.387 | 0.38722 | 0.14994 | 0.0006077 | 60 x $10^{-5}$ | 5.25 |
| Bed J | | Ora 9 | 2.9 | 3.8 | 1.31 | 0.539 | 0.387 | 0.39079 | 0.1527 | 0.0006250 | 62 x $10^{-5}$ | 5.4 |
| Bed L | | Ora 10 | 1.9 | 3.9 | 2.05 | 0.699 | 0.387 | 0.3938 | 0.15508 | 0.0032477 | 32 x $10^{-4}$ | 28.06 |
| Total | | | | | | 0.605 | | 0.390 | | | | |

## Petrophysical Parameters

The petrophysical parameters, the mean grain diameter, $d_{10}$ and $d_{60}$, (where $d_{60}$ and $d_{10}$ are the sieve diameters in (mm) for which 60% and 10% of the sample will pass respectively) of the studied sandstones are presented in Table 2 above.

The coefficient of uniformity is an indicator to the size, shape, distribution, packing and sorting of grains (Chilingar et al., 1963). Equation 4 was used to calculate the coefficient of uniformity. Higher coefficient uniformity indicates a large range of particle size, the lower the value of the coefficient of uniformity, the more uniform the grading of the aquifer material. Granular material with coefficient uniformity (η) less than 10 is regarded as uniformly graded, while granular material with coefficient uniformity (η) more than 10 is regarded as well-graded (Powrie, 2004). The coefficient of uniformity for the sandstone range from 1.11 – 3.00, inferring it is uniformly graded.

Porosity (η) is a dimensionless quantity with a magnitude less than one. It was calculated using equation 3 by Vukovic and Soro, 1992. It could be expressed in percentage (%) or in fraction. Porosity is a significant parameter considered in characterizing an aquifer or a reservoir. Fine-grained sediments exhibit higher porosities (η) than coarse-grained sediments because the number of contacts between fine grains tends to increase, leading to a looser packing, Salem (2001). The porosity values of the sandstone range from 0.504 to 0.903, with an average of 0.608. In natural sedimentary deposits, fine-grained sands tend to be more uniform and exist at higher porosities than coarse grained sands (Kezdi, 1974). Porosity of the sandstone ranges mainly from 0.5 to 0.7 with few sample reading above 0.7, that is between 50% - 70%. Whereas, the least estimated permeability is 3.74 and the highest is 724.55 m/day. Permeability was calculated using Equation 5 by kozeny – Carman. A very complex variation exist in the permeability of the studied sandstone. This may be the resultant effect of the several large planar, trough and herringbone cross stratification, erosion and pebble lagged surfaces prevalent in the Formation. There is a strong correlation between permeability and porosity and the associated regression equation is expressed, with a correlation coefficient $R^2 = 0.6795$ (Figure 23).

Permeability was correlated with a number of particle-size parameters. Scatter plots were generated to compare permeability with geometric mean diameters and poor correlation is observed as coefficient of correlation is $R^2 = 0.0061$. The average geometric mean diameter for the sample is 0.390 (Figure 24 and 25). Equation 1 was used to calculate the geometric mean diameter, while, equation 2 was for the geometric mean of rated size of adjacent sieves ($d_{ig}$).

Other particle size parameters correlated with permeability are $d_{10}$ and $d_{60}$, and poor correlation was observed. The grain size that passed through the 60 percentile is mainly fine sand to coarse silt, while, a range of granules to coarse silt passed through 10 percentile. Figures 26 and 27 are scatter plots of $d_{10}$ and $d_{60}$ of the sandstone samples. The $d_{10}$ diameter in millimeters has a correlation of $R^2 = 0.3156$ with permeability, while that of $d_{60}$ is $R^2 = 0.0015$.

The porosity values confirm the friability of the sandstone, and the complex variation of permeability results from the various sedimentary structures prevalent in the sandstone and the intermittent mudrapes overlying the cross-beds forming seals.

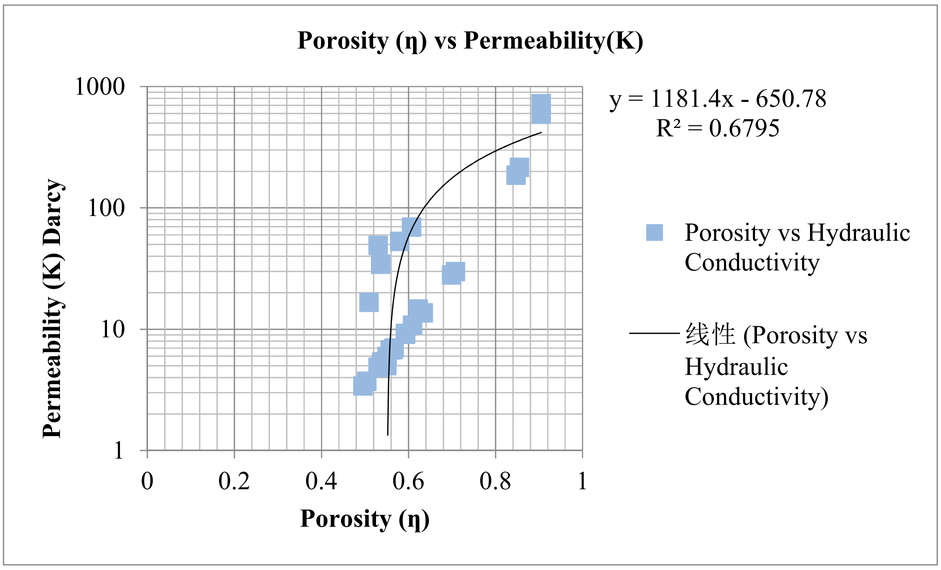


Figure 23: Plot of porosity(η) versus permeability(k).

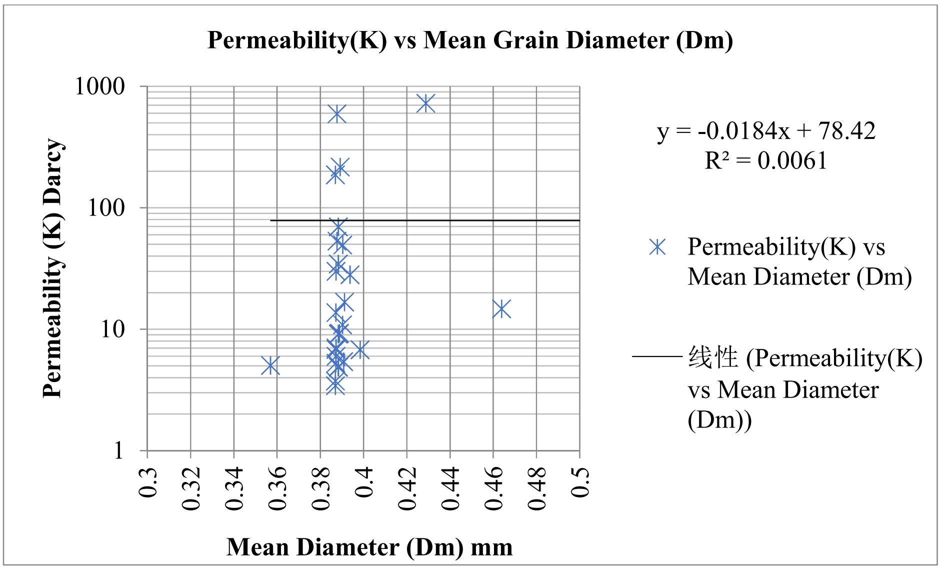


Figure 24: Plot of permeability(k) versus mean grain diameter(Dm).

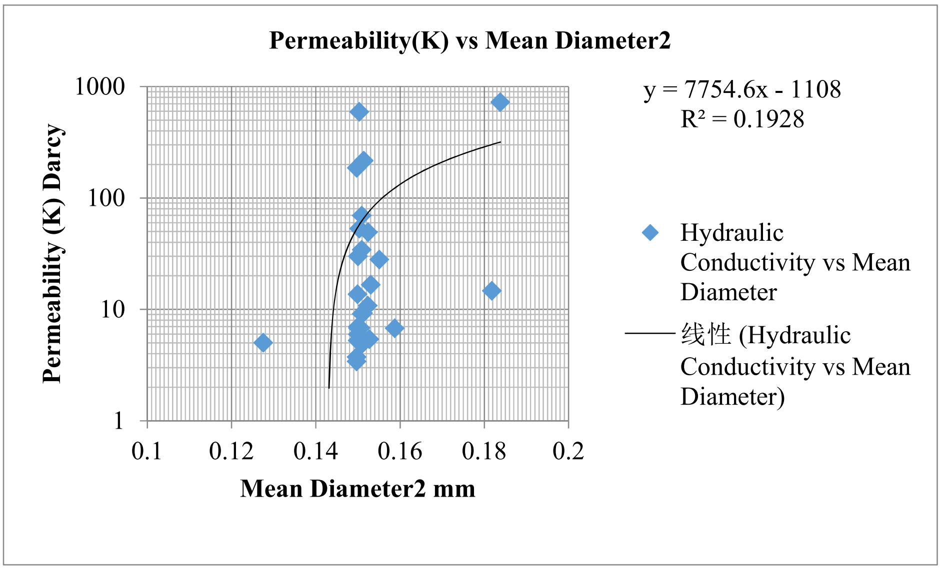


Figure 25: Plot of permeability(k) versus square of mean grain diameter ($D^2m$).

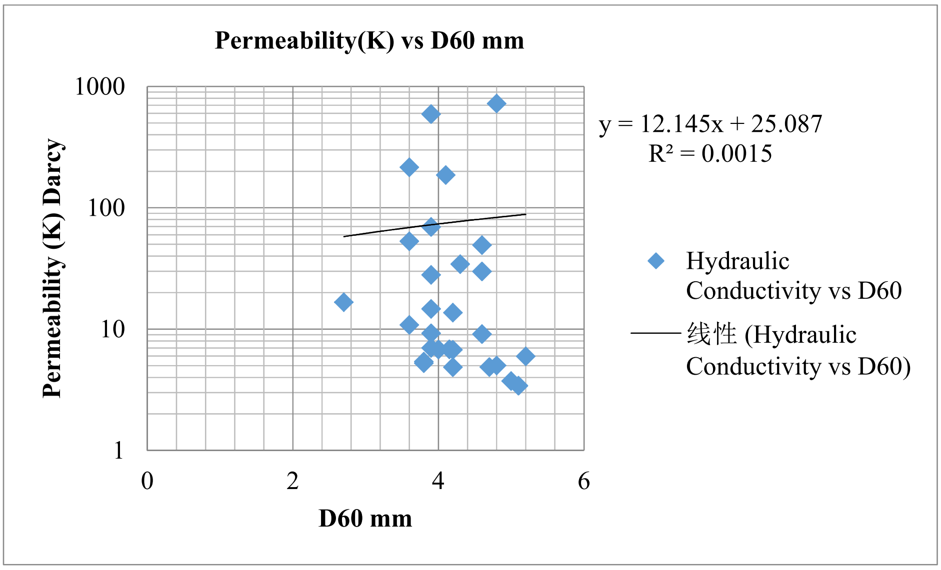


Figure 26: Plot of permeability(k) versus $D_{60}$ mm.

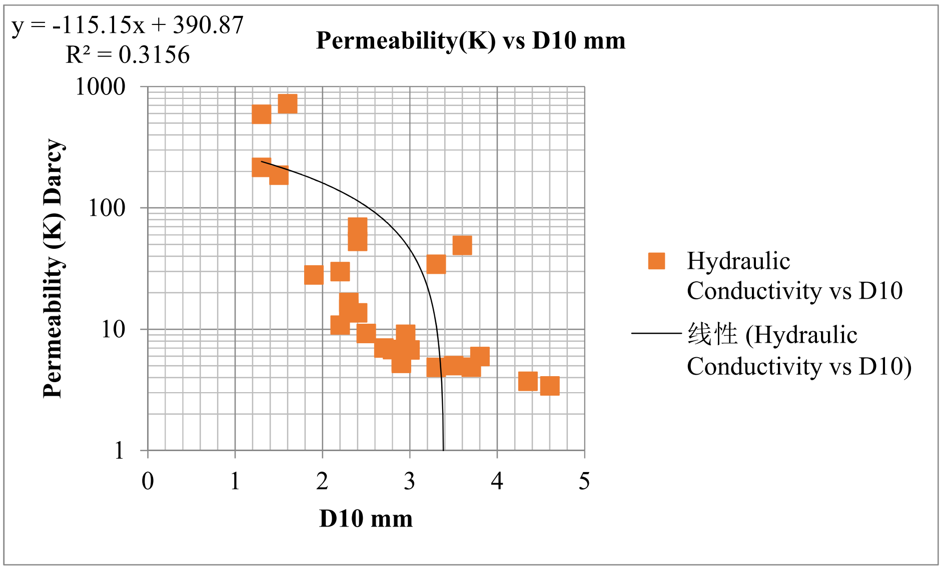


Figure 27: Plot of permeability(k) versus $D_{10}$ mm.

## Conclusion

The Campanian – Maastrichtian proto delta sediments in the Anambra Basin include the Nkporo Group, Mamu Formation, Ajali Formation and the Nsukka Formation. The Ajali Sandstone is sandwiched between the Mamu Formation and the Nsukka Formation - the lower and upper coal measures respectively. The sandstone is very friable due to lack of cement and several diagenetic influences, such as alteration, corrosion, dissolution at grain margins and contacts. These, in conjunction with some sedimentary structures, such as, planar, trough cross-beds, erosion surfaces, mud drapes, herringbone cross-stratification and textural characteristics impart the petrophysical properties of the Ajali Sandstone.

The Ajali Formations in the study area grain size distribution has an average Mean of 3.80, reflective of the very fine sand fraction for the sandstone and the Sorting is 0.92 which is moderately sorted.

The porosity of the sandstone is very high and ranges mainly from 50% - 70%, with a few above 70%. Whereas, the least estimated permeability is 3.74 m/day and the highest is 724.55 m/day. A very complex variation exist in the permeability of the studied sandstone which may be due to the occurrence of the several large planar, trough and herringbone cross stratification, erosion and pebble lagged surfaces prevalent in the Formation. There is a strong correlation between permeability and porosity and the associated regression equation is expressed, with a correlation coefficient $R^2 = 0.6795$

The plots of permeability with other grain size parameters such as, grain mean diameter, $d_{10}$ and $d_{60}$, show poor correlation.

## References

*[1] Akpofure, E., Etu-Efeotor, J.O. (2013a) Petrography of Ajali Sandstone in Ayogwiri – Fugar – Orame Area of Western Anambra Basin: Implication for diagenetic and depositional history. Journal of Environmental and Earth Sciences. Vol 3 No 5, p 104 - 113.*

*[2] Akpofure, E., Etu-Efeotor, J.O. ( 2013b) Influences of depositional environment on the sedimentary structures,*

*biostratigraphy and textural characteristics of Ajali Sandstone in Ayogwiri – Fugar – Orame Area of Western Anambra Basin. European Journal of Scientific Research, Volume 103, Issue 4.*
*[3] Akpofure, E. Akana, S.T. (2016) Palaeocurrent and Facies Analysis Of Ajali Sandstone In Western Anambra Basin, Nigeria. Journal of Africa Earth Sciences. (Elsevier) 118 (2016) 75 - 86*
*[4] Amajor, L.C. (1987) Palaeocurrent, petrography and provenance analysis of the Ajali sandstone (Upper Cretaceous). Southeastern Benue Trough, Nigeria. Sedimentary Geology, vol.54 p.47-60.*
*[5] Chilingar G.V., Main R., Sinnokrot A. (1963) Relationship between porosity, permeability and surface areas of sediments. Journal of Sedimentary Petrology, 33: 759–765*
*[6] Folk, R.L., Ward, W. (1957) Brazos river bar: a study of the significance of grain size parameters. Journal of Sedimentary Petrology, 27, 3-26.*
*[7] Hoque, M. and Ezepue, M.C. (1977) Petrology and palaeogeography of the Ajali Sandstone. Journal Mining Geology. 14, 16-27.*
*[8] Jones, H.A and Hockey, R.D. (1964) The geology of part of South-Western Nigeria. Explanation of 1:250,000 sheets nos.59 and 68. Bulletin Geological Survey Nigeria, 31, 101pp.*
*[9] Kezdi, A. (1974) Soil mechanics, Elsevier Scientific Publishing Company, Vol. 1, P. 49; Elsevier, New York.*
*[10] Kogbe, C.A. (1976) Palaeogeographic history of Nigeria from Albian times. In: Geology of Nigeria (Edited by C.A. Kogbe). Lagos, Nigeria: Elizabethan publishing.*
*[11] Ladipo, K.O. (1986a) Tidal shelf depositional model for Ajali Sandstone, Anambra Basin, Southern Nigeria. Journal of African Earth Sciences, Vol. 5, No 2, pp 177-185, Nio & A van Gelder eds.*
*[12] Ladipo, K.O. (1988a) Paleogeography, Sedimentation and Tectonics of the Upper Cretaceous Anambra basin, Southeastern Nigeria Journal of African Earth Sciences.,v.7, p.815-821.*
*[13] Ladipo, K.O. (1988b) Examples of Tidal current Periodicities from Upper Cretaceous Sandstone (Anambra Basin SE Nigeria). In Boer, P.L., Van, A. and Nio, S.D. (Eds). Tide Influenced Sedimentary Environments and Facies. D. Riedel Publ. Co., Dorgrecht, p,333-340.*
*[14] Nwajide, C.S. and Reijers, T.J.A. (1996) Sequence architecture in outcrops. Example from the Anambra Basin, Nigeria NAPE Bulletin, v.11, no.01, p.23-32.*
*[15] Powrie, W. (2004) Soil Mechanics: Concepts and Applications. 2nd Ed. Taylor & Francis 270 Madison Avenue, New York, NY 10016.*
*[16] Rahaman, M.A. (1976a) Review of the basement geology of South-Western Nigeria. In: C.A. Kogbe (Editor), Geology of Nigeria. Elizabethen Publishing. Lagos, pp. 41-58.*
*[17] Reyment, R.A. (1965) Aspects of Geology of Nigeria. Ibadan University Press, 133 pages, 18pl.*
*[18] Salem, H. S., 2001: Determination of Porosity, Formation Resistivity Factor, Archie Cementation Factor, and Pore Geometry Factor for a Glacial Aquifer, Energy Sources, 23:6, 589-596. http://dx.doi.org/10.1080/00908310152125238*
*[19] Simpson, A. (1955) The Nigerian coal field. The geology of parts of Onitsha, Owerri and Benue provinces. Geological Survey Of Nigeria Bulletin, no.24, 85p, 5pl.*
*[20] Tucker, M.E. (Ed) (1988) Techniques in Sedimentology. Blackwell Scientific Publications, Oxford, 394 pp.*
*[21] Visher, G.S. (1969) Grain size distributions and depositional processes: Journal of Sedimentary Petrology, v.39, pp. 1074-1106.*
*[22] Vukovic, M., and Soro, A., 1992, Determination of hydraulic conductivity of porous medla from grain-size composition: Water Resources Publications, Littleton, CO, 83 PP*